# Low-optical-pumping-threshold InGaAs/GaAs nano-ridge laser monolithically grown on 300 mm silicon substrate

Z. Ouyang,[1] E. M. B. Fahmy,[1] D. Colucci, [1,2] A. A. Yimam, [1] B. Kunert[2] and D. Van Thourhout[1]

[1] Gent University-imec, Photonics Research Group, INTEC department, iGent, Technologiepark-Zwijnaarde 126, 9052 Ghent, Belgium
[2] IMEC, Kapeldreef 75, 3001 Heverlee, Belgium

## Abstract

*The monolithic growth of III-V materials directly on a Si substrate is a promising approach for realizing complex silicon photonic integrated circuits (PICs) including sources and amplifiers. It remains challenging to realize practical, reliable and efficient light emitters however, due to defect formation during the epitaxial process. Exploiting the aspect ratio defect trapping (ART) technique and nano-ridge engineering (NRE), nano-ridges with high crystal quality were achieved. In earlier work we used etched gratings to create distributed feedback (DFB) lasers from these nano-ridges[1]. Here we deposited an amorphous silicon (a-Si) grating on the top of nano-ridge. Under pulsed optical pumping, ~ 2.8 kW/cm$^2$ lasing turn-on threshold was observed, more than 10 times smaller compared to etched grating devices. This low-optical-pumping-threshold again demonstrates the high quality of the epitaxial material and provides an alternative route towards realizing electrically-driven devices.*

## Introduction

Leveraging well-developed processes from the complementary metal-oxide semiconductors (CMOSs) industry, silicon photonics circuits incorporating various optical components, including high-efficiency grating couplers, high-response-speed photodetectors and excellent modulators[2-4] are now widely studied. However, the lack of a high-performance laser is a main bottleneck for further development of the silicon photonic platform. Direct-bandgap III-V semiconductors are the promising candidate for realizing a practical and compact light source but not easy to integrated on silicon. Several methods, including flip-chip, bonding, transfer printing and direct epitaxy of III-V materials utilizing a buffer layer[5-8], were explored to achieve this but all have their limitations. The novel nano-ridge engineering (NRE) technique[9-10] has been shown to enable the growth of high-quality III-V material directly on Si substrates without any buffer layer, and compared to other methods shows advantages in terms of device scalability, integration density and cost.

In our previous work, although the nano-ridge cavity with etching grating had been realized, the threshold of these devices were still high[1]. One of the reasons is that the etched structure caused the damage to InGaP passivation layer, which introduced more surface recombination centers. It is necessary to understand the non-radiative surface recombination mechanism and reduce the damage to passivation for improving laser performance further. Therefore, in this work, high-refractive-index, but ‘weak’ and small a-Si grating were deposited on the top of nano-ridge rather than etched grating inside nano-ridge. The design of a-Si grating considered the light interaction with grating and

more mode overlap with quantum wells into account, which contributed to form nano-ridge cavity with behaving low lasing turn-on.

# Experiment

## 1. GaAs nano-ridge epitaxial growth

The box-shaped nano-ridges with high crystal quality and large III/V material volume were grown by metal organic vapor phase epitaxy (MOVPE) on a silicon substrate containing narrow trenches patterned in a $SiO_2$ layer. The details of the epitaxy process can be found in previous reports[1,9-10]. Figure 1(a)-(b) give the image of the overall structure, the InGaAs quantum wells inside nano-ridge and the trench part of the nano-ridge[1]. Figure 1(c) shows that the oxide sidewall effectively blocks threading dislocations, avoiding extension of these defects into the large III/V material volume above the trench, as shown in Figure 1(b). Figure 1(d) and (e) show a top-view of nano-ridges with different sizes and a cross-section view of a nano-ridge with 60 nm trench size (485 nm-high and 411 nm-width nano-ridge). All of the nano-ridges in these two figures were used to design nano-ridge lasers with a top a-Si grating. The basic transverse electric (TE)-like mode in a 485 nm-high nano-ridge without and with a-Si grating on the top are given in figure 1(f) and (g). Both TE modes exhibit high confinement and negligible substrate leakage loss, 0.46 dB/cm and 0.21 dB/cm, respectively. This low substrate leakage loss contributes to a low-optical-pumping-threshold.

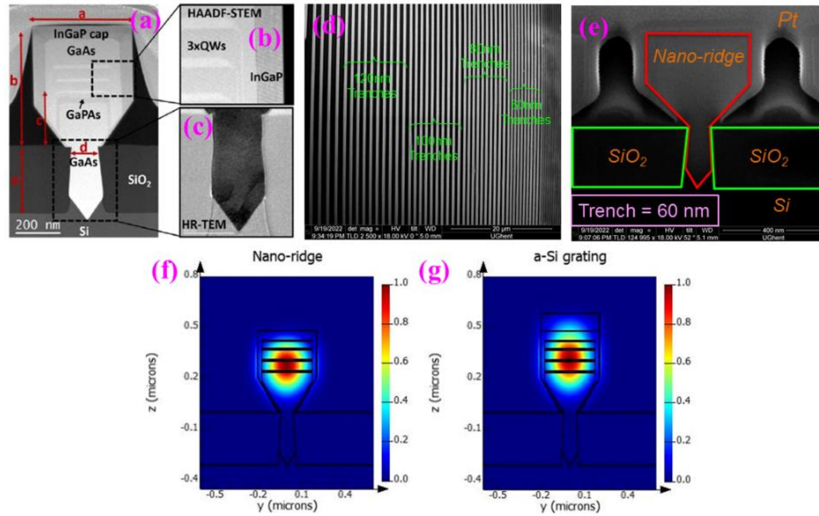


Figure 1(a) The HAADF-STEM image of nano-ridge structure from reference [1]. (b) Zoomed-in HAADF-STEM image of the quantum wells part in (a). (c) The HR-TEM image of the trench region from reference [1]. (d) Top view SEM image of nano-ridge array with trench width from 60 nm to 120 nm. (e) Cross-section SEM image of 485 nm-high nano-ridge (with 60 nm trench width). The basic transverse electric (TE)-like mode in a 485 nm-high nano-ridge without (f) and with (g) a-Si grating on the top.

## 2. Photoluminescence and fabrication process

The material quality of the nano-ridge was characterized by photoluminescence measurements at the room temperature. The nano-ridges were excited by a 532 nm continuous-wave (CW) solid state diode laser (MGL-FN-532-1.5W model, Changchun New Industries Optoelectronics Technology Co., Ltd). The emission from the nano-ridges was collected and detected with a monochromator (Oriel MS257 1/4m, Newport) and a thermo-electric-cooled InGaAs detector (Oriel, 70328NS model, Newport). Figure 2(a) presents the normalized photoluminescence spectrum from nano-ridges with

different trench sizes under 4.20 W/cm$^2$ pumping power density. The photoluminescence spectrum contains a broad peak extending from 1000 nm to 1060 nm.

After optimizing the trade-off between light interaction with the a-Si grating on the top of nano-ridge and mode confinement in quantum wells with a 3D-finite difference time domain (3D-FDTD) solver, the 100 nm a-Si thin film was deposited on nano-ridge chips by plasma-enhanced chemical vapor deposition (Advanced Vacuum Vision 310 PECVD, Plasma-Therm) after aceton, isopropyl alcohol (IPA) and DI water cleaning. Due to the reaction between the a-Si layer and the developer (AZ400K:DI water = 1:3) of hydrogen silsesquioxane resist (HSQ, Dow Corning), ~ 50 nm cured benzocyclobutene (BCB) was added as protection layer before ~ 150 nm HSQ resist spin coating and the electron beam lithography (EBL, Voyager, Raith). Then, 800 grating periods in total were patterned into HSQ resist after EBL and the development. The patterned structures were transferred from HSQ resist to the a-Si layer by reactive-ion etching of the BCB layer and the a-Si layer with $SF_6/O_2$ and $CF_4/H_2/SF_6$, respectively. The successfully fabricated devices, including a 200-period second-order grating added at one side to couple light out, are shown in Figure 2(b). Figure 2(c) present zoomed-in tilted scanning electron microscope (SEM) images. Figure 2(d) shows the vertical sidewall and smooth surface of the a-Si grating, which benefits the low-optical-pumping-threshold.

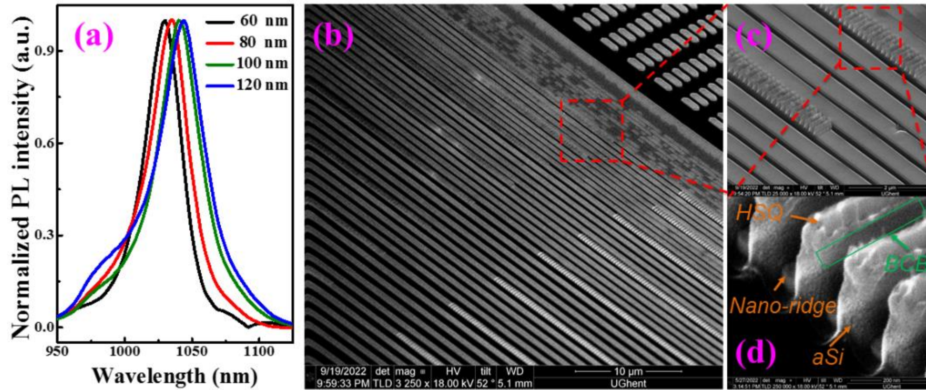


Figure 2(a) Normalized room-temperature photoluminescence spectra of nano-ridges with different trench widths. (b) Tilted SEM image of all DFB lasers with different trench sizes. (c) Zoomed-in tilted SEM image of DFB laser with 60 nm trench size. (d) Zoomed-in tilted SEM image of a-Si grating on the top of 485 nm-high nano-ridge (with 60 nm trench size.).

## Results and discussion

The devices were excited by a Nd:YAG 532-nm nanosecond pulsed laser (7 ns pulse width, 938 HZ repetition rate, NL200 series laser, EKSPLA, Lithuania) at room temperature. The emission from the devices was collected and detected with the same monochromator and InGaAs detector, as mentioned before. Figure 3(a) shows a microscope picture of a full array of devices excited simultaneously by a 200 μm-radius pump spot. For single device characterization, a rectangle slit was utilized to control the pump spot size, as presented in Figure 3(b). Figure 3(c) shows the photoluminescence spectrum of the DFB laser based on 485 nm-high nano-ridges, 100 nm-high a-Si grating and 165 nm a-Si grating period under different 532nm pulsed pumping power densities. The 1028 nm lasing peak becomes apparent when the pumping density reaches 11 kW/cm$^2$ and the peak intensity increases strongly with the further increase of the pumping density. At the pumping power density of 61 kW/cm$^2$, the lasing peak reaches more than 22 dB side-mode suppression ratio, demonstrating excellent laser performance. The line with of the laser is 4.5 nm, limited by the input slit width setting. A clear change of slope

in the light in (pumping power density) - light out (integrated photoluminescence intensity) curve on linear and logarithmic (inset) scale from the same DFB laser illustrates lasing turn-on behavior, as shown in Figure 3(d). Figure 3(e) shows the photoluminescence spectrum of the DFB laser based on nano-ridges with 120 nm trench size (539 nm-high and 582 nm-width nano-ridge), 100 nm-high a-Si grating and 161 nm a-Si grating period under 2.8 kW/cm$^2$ pulsed pumping power density and the 1044 nm lasing peak appears. This threshold value is more than 10 times smaller than that reported earlier[1]. This is because the a-Si grating deposited on the top of nano-ridge avoids any damage to the InGaP surface passivation layer and does not induce surface recombination centers during the etching process.

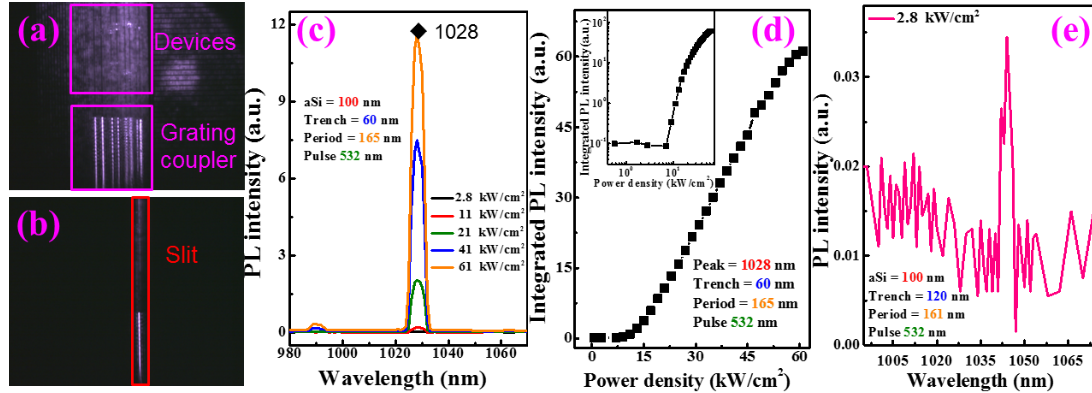


Figure 3(a) The image of all excited DFB laser with different trench sizes under 532 nm pulsed pumping. (b) The image of one excited DFB laser with slit under 532 nm pulsed pumping. (c) Photoluminescence spectrum from the DFB laser with 60 nm trench size under different 532 nm pulsed pumping densities. (d) Light in -Light out curve on linear and logarithmic (inset) scale of the DFB laser with 60 nm trench size. (e) Photoluminescence spectrum from the DFB laser with 120 nm trench size under 2.8 kW/cm$^2$ pulsed pumping density.

## Conclusion

In conclusion, in order to achieve low-optical-pumping-threshold nano-ridge laser monolithically grown on a standard 300-mm Si wafer, 100nm-high a-Si grating was deposited on the top of nano-ridge. Room temperature measurement shows clear laser operation with a side-mode-suppression ratio better than 22 dB side-mode suppression ratio and 2.8 kW/cm$^2$ lasing threshold. This lasing threshold is more than 10 times smaller than DFB laser with etched grating, which is ascribed to a-Si grating deposition on the top avoiding damaging InGaP passivation cladding and introducing more surface recombination paths. This low-optical-pumping-threshold nano-ridge laser demonstration proves high quality of the III-V-on-silicon epitaxial material again and open up the road towards achieving high-performance electrically-driven devices.

## Acknowledgment

This project has received funding from the European Union's Horizon 2020 research and innovation programme under grant agreement No. 884963 (ERC AdG NARIOS) and China Scholarship Council.

## References

[1] Y. Shi, Z. Wang, J.V. Campenhout, et al, "Optical pumped InGaAs/GaAs nano-ridge laser epitaxially grown on a standard 300-mm Si wafer", Optica, vol. 4, 1468-1473, 2017.

[2] R. marchetti, C. Lacava, A. khokhar, et al, “High-efficiency grating-couplers:demonstration of a new design strategy”, Scientific Report, vol. 7, 16670:1-8, 2017.
[3] N. Youngblood, C. Chen, S. J. Koester and M. Li, “Waveguide-integrated black phosphorus photodetector with high responsivity and low dark current”, Nature Photonic, vol. 9, 247-252, 2015.
[4] Y. Terada, K. Kondo, R. Abe and T. Baba, “Full C-band Si photonic crystal waveguide modulator”, Optics Letter, vol. 42, 5110-5112, 2017.
[5] H. Lu, J. Lee, Y. Zhao et al, “Flip-chip integration of tilted VCSELs onto a silicon photonic integrated circuit”, Optics Express, vol. 42, 5110-5112, 2017.
[6] M. R. Billah, M. Blaicher, T. Hoose, et al, “Hybrid integration of silicon photonics circuits and InP lasers by photonic wire bonding”, Optica, vol. 5, 876-883, 2018.
[7] J. Zhang, G. Muliuk, J. Juvert, et al, “III-V-on-Si photonic integrated circuits realized using micro-transfer-printing”, APL Photonics, vol. 4, 11803:1-10, 2019.
[8] J. Yang, P. Jurczak, F. Cui, et al, “Thin Ge buffer layer on silicon for integration of III-V on silicon”, Journal of crystal growth, vol. 514, 109-113, 2019.
[9] B. Kunert, W. Guo, Y. Mols, et al, “Integration of III/V Hetero-Structures by Selective Area Growth on Si for Nano- and Optoelectronics”, ECS Transactions, vol. 35, 679-681, 2010.
[10] B. Kunert, R. Alcotte, Y. Mols, et al, “Application of an Sb Surfactant in InGaAs Nano-ridge Engineering on 300 mm Silicon Substrates”, Crystal Growth and Design, vol. 21, 1657-1665, 2021.
[11] D. Colucci, M. Barysgbujiva, Y. Shi, et al, “Unique design approach to realize an O-band laser monolithically integrated on 300mm Si substrate by nano-ridge engineering”, Optics Express, vol. 30, 13510-13521, 2021.